Langmuir

Stable Oligomeric Clusters of Gold Nanoparticles: Preparation, Size Distribution, Derivatization, and Physical and Biological Properties

Oliver Smithies,*,† Marlon Lawrence,† Anze Testen,§ Lloyd P. Horne,‡,∥ Jennifer Wilder,† Michael Altenburg,† Ben Bleasdale,†,⊥ Nobuyo Maeda,† and Tilen Koklic*,§

†Department of Pathology and Laboratory Medicine, and ‡Department of Chemistry, University of North Carolina at Chapel Hill, Chapel Hill, North Carolina 27599, United States
§Condensed Matter Physics Department, Laboratory of Biophysics, "Jožef Stefan" Institute, Ljubljana 1001, Slovenia

Ⓢ Supporting Information

ABSTRACT: Reducing dilute aqueous $HAuCl_4$ with NaSCN under alkaline conditions produces 2−3 nm diameter yellow nanoparticles without the addition of extraneous capping agents. We here describe two very simple methods for producing highly stable oligomeric grape-like clusters (oligoclusters) of these small nanoparticles. The oligoclusters have well-controlled diameters ranging from ∼5 to ∼30 nm, depending mainly on the number of subunits in the cluster. Our first ["delay-time"] method controls the size of the oligoclusters by varying from seconds to hours the delay time between making the $HAuCl_4$ alkaline and adding the reducing agent, NaSCN. Our second ["add-on"] method controls size by using yellow nanoparticles as seeds onto which varying amounts of gold derived from "hydroxylated gold", $Na^+[Au(OH_{4-x})Cl_x]^-$, are added-on catalytically in the presence of NaSCN. Possible reaction mechanisms and a simple kinetic model fitting the data are discussed. The crude oligocluster preparations have narrow size distributions, and for most purposes do not require fractionation. The oligoclusters do not aggregate after ∼300-fold centrifugal-filter concentration, and at this high concentration are easily derivatized with a variety of thiol-containing reagents. This allows rare or expensive derivatizing reagents to be used economically. Unlike conventional glutathione-capped nanoparticles of comparable gold content, large oligoclusters derivatized with glutathione do not aggregate at high concentrations in phosphate-buffered saline (PBS) or in the circulation when injected into mice. Mice receiving them intravenously show no visible signs of distress. Their sizes can be made small enough to allow their excretion in the urine or large enough to prevent them from crossing capillary basement membranes. They are directly visible in electron micrographs without enhancement, and can model the biological fate of protein-like macromolecules with controlled sizes and charges. The ease of derivatizing the oligoclusters makes them potentially useful for presenting pharmacological agents to different tissues while controlling escape of the reagents from the circulation.
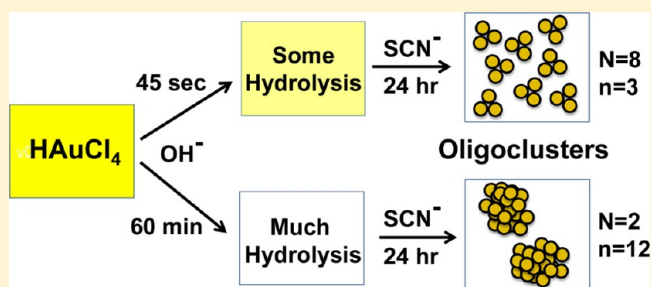
1. INTRODUCTION

The ability to locate and track the movement of proteins and other macromolecules is indispensable for understanding how multiple organ systems function. At the level of tissues and cells, tracers that are intrinsically fluorescent have been used with great success.[1] At the subcellular level, transmission electron microscopy (TEM) in conjunction with nanoparticle-tagged antibodies is likewise successful, although difficult to quantify. The use of intrinsically electron-dense macromolecules facilitates quantification, as exemplified by studies of the renal disposal of intravenously injected ferritin.[2−4] Gold nanoparticles offer a more electron-dense substitute for ferritin and can be made in different sizes. An important additional merit is that they can be prepared with a variety of surface coatings, which modulate their physical and biological properties[5,6] and enable them to deliver pharmaceuticals to desired locations.[7−9] With these factors in mind, we set out to prepare gold nanoparticles that meet the following criteria: they should

be nontoxic and should not aggregate at high concentrations in phosphate buffered saline (PBS) or in the circulation after intravenous injection in mice; they should be visible in TEM images without enhancement; they should be available in physiologically relevant sizes; the physiologically different particles should be recognizably different in TEM images enabling useful experiments with mixtures of differently sized particles; their surface coats should be changeable to allow control of their behavior in vivo; and they should have hydrodynamic sizes covering a range that determines their escape from the circulation and their excretion by the kidney.

Reducing $HAuCl_4$ with $NaBH_4$ and capping with glutathione (GSH), following variations of the Schaaff procedure,[10] allows the production of nanoparticles with increasing core diameters

and hydrodynamic radii. However, the resulting GSH-capped nanoparticles agglutinate in PBS when their hydrodynamic radii are significantly larger than that of albumin. In attempting to overcome this aggregation problem, we tested a method described previously[11,12] in which dilute aqueous $HAuCl_4$ is reduced with NaSCN under alkaline conditions. As originally described, the NaSCN method produces 2−3 nm diameter yellow nanoparticles. Here, we describe two very simple modifications of the NaSCN method that yield highly stable grape-like clusters (hereafter called "oligoclusters"), which can be made large and still meet our design criteria. The oligoclusters are comprised of variable numbers of the yellow nanoparticle subunits. The number of subunits in the oligoclusters determines their TEM sizes; the agents used for coating the oligoclusters determine their resistance to aggregation and modulate their hydrodynamic sizes and biological properties. Our oligoclusters enable (by direct visualization with the electron microscope) studies of the fates of macromolecules of different sizes and with different coats after introduction into the circulation. Studies at the molecular level of the permeation of the oligoclusters into and through the kidney glomerular basement membrane (GBM), and uptake by the proximal tubules, are readily accomplished, as are studies of the effects of size and coat on their clearance by the spleen and liver.

2. EXPERIMENTAL SECTION

2.1. Chemicals. Most chemicals (at least ACS reagent grade) were purchased from standard sources and used as received. For convenience in preparation and to facilitate varying reaction volumes, several stock solutions were made as molal (gram moles per kg of solvent) rather than as molar (gram moles per liter of solution). Likewise, the stock solution of ∼25 mM gold chloride was made from a 1 g vial of G4022 Sigma-Aldrich $HAuCl_4 \cdot xH_2O$ plus 100 g of H_2O. Bovine serum albumin (Sigma-Aldrich A2153, ≥96%), bovine IgG (Sigma-Aldrich G5009, ≥99%), cytochrome c from equine heart (Sigma-Aldrich C2506, ≥95%), and egg white ovalbumin (MP Biochemicals 95052, ≥80%) were further purified by gel permeation chromatography prior to use. Peptides synthesized to our order by GenScript (Piscataway, NJ) were used as received. Water was purified to 10−18 MΩ cm for inorganics and free from particulates >0.1 μm with a Type I water system (LBDRP1202, Continental Water Systems Corp., Lubbock, TX).

2.2. A Delay-Time Procedure for Synthesizing Oligoclusters of Gold Nanoparticles. The "delay-time" procedure for a 70 mL reaction was typically carried out in a 125 mL Wheaton glass bottle with reagents added in the following order: (a) 59.5 g of H_2O; (b) 7 mL of 0.1 molal borax ($Na_2B_4O_7 \cdot 10H_2O$: final concentration 10 mM); (c) 2.8 mL of ∼25 mM gold chloride ($HAuCl_4$: final concentration 1 mM) added rapidly with brief vigorous mixing; (d) after a chosen delay time (1 s to several hours) 700 μL of 1 molal NaSCN (final concentration 10 mM) added rapidly with brief vigorous mixing. The resulting mix was kept overnight to ensure completion of the reduction. Reaction volumes were varied by scaling all individual volumes proportionately. Fifteen milliliter reactions were carried out in 20 mL Fisher scintillation vials.

2.3. An Add-On Procedure for Synthesizing Oligoclusters Using Nanoparticles as Seeds. The "add-on" procedure requires the preparation of two stock solutions: (a) a 1 mM solution of "hydroxylated gold" (HG), and (b) a 1 mM solution of seeds. Preparation of the HG was typically carried out in a 125 mL Wheaton glass bottle with reagents added in the following order: 59.5 g of H_2O; 7 mL of 0.1 molal borax to give a final concentration of 10 mM; 2.8 mL of ∼25 mM $HAuCl_4$ added rapidly with brief vigorous mixing to give a final concentration of 1 mM. The resulting mix was kept at least a day to allow the hydroxylation reaction to approach equilibrium; thereafter, the stock solution of HG could be stored for weeks for

future use without further manipulations. Stock solutions of seeds (final gold concentration 1 mM) were prepared at least a day in advance using the delay-time procedure described above, typically with a 30 s delay time. The crude stock solutions of seeds remained usable for weeks thereafter without purification. In some experiments, longer (or shorter) delay times were used to increase (or decrease) the size of seeds. A small amount of gold precipitate eventually develops in seed stock solutions prepared with delay times <20 s, but is easily removed by centrifugation or decantation.

The add-on method controls the size of the oligoclusters by varying the ratio of seeds to HG, taking advantage of our finding that completely hydroxylated gold, $NaAu(OH)_4$, is not directly reducible by NaSCN, but that in the presence of nanoparticle seeds it is reduced. Add-on reactions were carried out by mixing the stock solutions of 1 mM seeds and 1 mM HG in various ratios and adding 1 M Na SCN to give a final concentration of 10 mM, assuming that the seed stock solution already contains 10 mM NaSCN. For example, a 1:1 reaction mix was made by adding 9 mL of HG to 9 mL of seed stock solution followed by the addition of 90 μL of 1 M NaSCN; a 1:4 mix contained 16 mL of HG, 4 mL of seed stock solution, and 160 μL of 1 M NaSCN. Reaction mixes were kept overnight after the addition of NaSCN to allow completion of the reduction. The numbers of subunits in the final oligoclusters, and the overall size of the oligoclusters, increased as the proportion of seeds in the mixture was decreased, as illustrated below. Overall reaction volumes were varied by scaling all individual volumes proportionally.

2.4. Derivatization of Oligoclusters. To derivatize the oligoclusters, 70 mL of crude mix prepared as described above was first concentrated to ∼250 μL with a 30 kDa cutoff Centricon Plus-70 (Millipore) centrifugal filter followed by the addition of 0.5 molal glutathione (154 mg of GSH per mL of 0.5 molal Na_2CO_3), or one of the thiols discussed below, to give a final concentration of 50 mM. Because the volume of the reactants is small at this stage (∼1/300th of the initial volume), rare or expensive derivatizing thiols can be used at concentrations (not necessarily as high as 50 mM) that enable efficient ligand exchange without incurring excessive costs. The derivatized oligoclusters were then washed by diluting the concentrated reaction mixture with ∼50 mL of H_2O or phosphate buffered saline (PBS) and reconcentrating the mixture to ∼250 μL with the centrifugal filter. The final concentrates of oligoclusters when diluted 1/1000 typically give optical densities at 260 nm ranging from 0.5 (for 1 s delay-time preparations) to 1.7 (60 min delay time), and contain up to 0.1 mg of gold per μL.

2.5. Electrophoresis. Polyacrylamide gel electrophoresis was with 15 slot mini-protean TGX 4-20% gradient gels (Bio-Rad, Hercules CA). Load volumes were 15 μL of a mixture typically containing 20% glycerol, ∼0.05% bromphenol blue, with GSH (50 mM GSH dissolved in 50 mM Na_2CO_3) or without GSH (50 mM $NaHCO_3$), with or without PBS. Colored images of the gels were obtained by scanning with an Epson Perfection 3170 scanner in the 24 bit RGB reflective mode; the blue component after RGB split was used for black and white images.

2.6. Electron Microscopy. Samples of oligoclusters were prepared for transmission electron microscopy (TEM) by placing 1 μL of the sample (diluted 1/200 in ultrafiltered water) on a grid with a carbon-coated support film that had been recently treated with glow discharge. To reduce undetectable sampling biases, the grids were allowed to dry without blotting or rinsing. Equal amounts of each preparation were spread on the grids; equal areas of the grids were examined at three or four different places; and particles were counted at four different magnifications. Most images were taken using a Zeiss TEM 910 operating at 80 kV. Size distribution analyses of the oligoclusters were obtained using ImageJ (vers. 1.46r) software available from the National Institutes of Health at http://rsb.info.nih.gov/ij/. Because some of the clusters are not spherical, minimum (d_{min}) and maximum diameters (d_{max}) were measured, and geometric averages ($d_g = (d_{min}d_{max})^{1/2}$) of both diameters were calculated (Feret diameters), which approximates the equivalent circular diameter. Feret diameters were used in analyzing the size distributions. High-resolution images

were taken using a JEOL 2010F HRTEM operating at 200 kV with a 2K × 2K Gatan CCD bottom mount camera.

2.7. Gel Permeation Chromatography. A high-resolution Superdex 200-10/300 gel filtration column (GE Healthcare Life Sciences, Piscataway, NJ) with a separation range for proteins of molecular weights between 10 000 and 600 000 was used for determining partition coefficients (K_d) and hydrodynamic radii (R_h), with PBS as the eluent. Analytic sample volumes were 180 μL with flow rates of 15 mL/h. Fraction sizes were 0.5 mL. The column was calibrated with proteins of known molecular weights and R_h (equine cytochrome c, egg white albumin, bovine serum albumin, and bovine immunoglobulin) and with acetone. Absorption at 260 nm was used to detect proteins and oligoclusters in the column eluates.

2.8. Animal Experiments. For determination of urinary excretion of injected oligoclusters, adult male C57Bl/6J mice that had been drinking a 3% glucose, 0.77% saccharin mix overnight to increase urine flow[13] were given 100 μL of concentrated GSH-modified oligoclusters in PBS by tail vein injection using standard restraints without anesthesia. At appropriate times thereafter (see Results and Discussion), the mice were euthanized by exposure to a high concentration of isofluorane vapor followed by cervical dislocation. Urine was collected by needle from their bladders, diluted at least 10-fold with PBS, and then filter-concentrated to a constant volume prior to electrophoresis.

For electron microscopic studies of renal glomeruli after injection of oligoclusters, mice were anesthetized with 5% isofluorane/air mixtures, the left kidney was exposed via an abdominal incision, and a suture was placed in preparation for rapid ligation of the renal pedicle. Concentrated nanoclusters were injected upstream into the superior mesenteric artery and thence (via the downstream renal arteries) into the glomeruli.[14] Ligation was performed in less than a second, followed by subcapsular injection of 100 μL of a modified form of Karnovsky's fixative (2% paraformaldehyde/2.5% glutaraldehyde/0.15 M sodium phosphate, pH 7.4) and excision of the kidney. The mice were then euthanized by cervical dislocation, and other organs were harvested for study. All animal experiments were carried out under protocols approved by the University of North Carolina Institutional Animal Care and Use Committee.

3. RESULTS AND DISCUSSION

Initial experiments using the reduction of HAuCl$_4$ by NaBH$_4$ in the presence of GSH showed that the resulting GSH-capped nanoparticles agglutinated in PBS when their hydrodynamic radii were significantly larger than that of albumin. The larger nanoparticles also agglutinated when in plasma or after injection into mice. These results prompted us to test sodium thiocyanate (NaSCN) as an alternative reductant, which is known to form stable ~2.6 nm diameter yellow nanoparticles without requiring any additional capping agent.[11,12] These tests showed that when the time between making the HAuCl$_4$ alkaline and the addition of NaSCN was lengthened, the sizes of the product increased, as judged by gradient polyacrylamide electrophoresis, although their color remained yellow. In contrast, the nanoparticles formed by the reduction of gold chloride with NaBH$_4$ change color as their sizes increase. This apparent paradox was resolved when TEM inspection of the NaSCN-reduced products showed that the particles formed with longer delay times were oligoclusters of small yellow subunits. This observation allowed us to develop our "delay-time" procedure, which uses time as a simple means of controlling the sizes of the oligoclusters.

3.1. Delay-Time Procedure. Briefly, as detailed in the Experimental Section, a 25 mM solution of gold chloride (HAuCl$_4$) is added to a 10 mM solution of borax, with brief vigorous mixing, to give a final HAuCl$_4$ concentration of 1 mM. After a carefully controlled delay time, during which [AuCl$_4$]$^-$

is rapidly being hydrolyzed,[15,16] NaSCN is added as a reductant, again with brief vigorous mixing, to give a final NaSCN concentration of 10 mM. The reaction mixture is kept at room temperature at least overnight to ensure completion of the reduction, after which the resulting oligoclusters can be filter-concentrated.

The order of addition of solutions is critical, for reasons discussed below, and longer delay times before adding the NaSCN to the alkaline reaction mixture give larger oligoclusters. The reaction is highly sensitive to variations in pH. Accordingly, we chose borax as the buffer, rather than the carbonate used by Baschong et al.,[12] because borax in aqueous solution yields an equimolar mixture of boric acid and sodium borate and therefore has a pH of 9.18 (the pK of boric acid) without adjustment, and because at the resulting final reaction pH (~8.6) reduction of [AuCl$_4$]$^-$ with NaSCN leads to the desired product with negligible amounts of precipitated gold. However, the reaction can also be accomplished with carbonate or phosphate buffers.

The crude preparations of oligomeric nanoparticles, concentrated or unconcentrated, can be kept in their mother liquor for weeks without developing more than trace amounts of precipitated gold when the delay times are ≥20 s. However, the reaction does not go to completion when delay times are <20 s, and some gold precipitate develops over time from the incompletely reacted material. Consequently, for storage, the short delay-time oligoclusters are best filter-concentrated ≥100-fold to remove >99% of the residual reactants while still leaving the oligoclusters in the final reaction mother liquor in which they are stable; they do not need to be washed. [As detailed below, an important feature of the NaSCN-derived oligoclusters is their resistance to aggregation when highly concentrated.]

Figure 1 compares the migration in a polyacrylamide gradient gel of GSH-derivatized oligoclusters obtained with delay times ranging from 0 to 60 min.

The derivatized oligoclusters migrate with progressively decreasing mobilities in the gradient gel as the delay time lengthens, showing that they have become larger and/or have less charge. In dilute agar-gel electrophoresis, however, the mobilities of the oligoclusters obtained with 15 and 45 s delay times were indistinguishable (data not shown). This indicates that the changes in polyacrylamide gel mobilities are probably mainly due to differences in the sizes of the oligoclusters, rather than in their charges. The longer delay-time oligoclusters appear notably darker in the image, which is also indicative of an increase in size, because previous work has shown that the extinction coefficient of gold nanoparticles increases in proportion to particle size.[17]

3.2. Shapes and Sizes of the Oligoclusters. The general shapes and size distributions of the oligoclusters made with different delay times were determined by transmission electron microscopy (TEM). Figure 2 illustrates images obtained with GSH-derivatized preparations made with delay times of 15 and 135 s. Figure 2A and B shows the most obvious difference, that the shorter delay-time preparation consists largely of monomers while the longer delay-time preparation consists of clusters of subunits (oligoclusters). As illustrated in Figure 2C and D, the mean diameters of the clusters increased about 3-fold when the delay time increased 9-fold. Interestingly, the distribution of core sizes in the largely monomeric 15 s preparation is close to log-normal, while the distribution of sizes in the oligo-clustered 135 s preparation is close to normal. This difference suggests
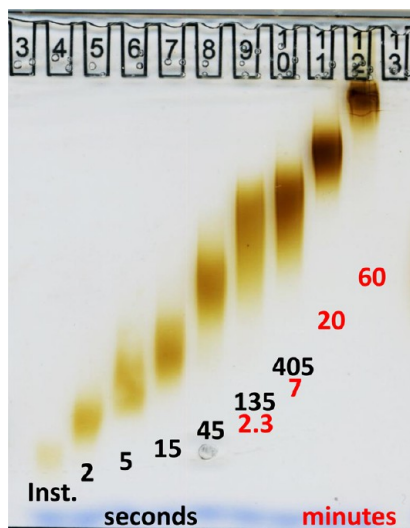
Figure 1. Polyacrylamide gradient gel electrophoresis of oligoclusters formed after different delay times between making the HAuCl$_4$ alkaline and the addition of NaSCN. The delay times used in preparing the oligoclusters are listed in seconds and minutes in black and red, respectively. "Inst." indicates that the NaSCN was added to the reaction mix at the same time as adding the borax (instantaneously). The samples used for the electrophoresis were from stored preparations that had been GSH-derivatized earlier, washed with water, and reconcentrated. Equal volumes of samples were loaded.

that the reactions determining the sizes of the monomers are different from those determining the number of monomers in a cluster.

Figure 3 presents a summary of the size distributions and TEM images of all of the preparations that were used for the electrophoresis experiment illustrated in Figure 1.

The preparations made with short delay times (2−15 s) have sizes comparable to those of the yellow nanoparticles described by Baschong et al.[12] The longer delay-time preparations, in contrast, are clearly grape-like clusters of subunits which have sizes comparable to those of the yellow nanoparticles. This accounts for the oligoclusters being yellow, even though their overall sizes are similar to those of red or blue colored nanoparticles formed by reducing HAuCl$_4$ with citrate or NaBH$_4$. The contours of the larger oligoclusters are irregular, and the edges of their TEM images are not sharp. In contrast, citrate or NaBH$_4$ nanoparticles have smooth contours. The irregularity of the oligoclusters may contribute to their resistance to aggregation (see below). The heavy black line in the figure is a best-fit ($R^2 = 0.973$) three-parameter equation, which describes how the diameters in nanometers (f) of the cores of the oligoclusters are related to the delay time in seconds (t) used in preparing them; t can vary from zero to infinity. In the three-parameter equation, [$f = y_0 + a \cdot (1 - \exp(-b \cdot t))$], y_0 is the observed minimum diameter of the cores (3.5 nm), a is the maximum observed increase in core diameters (20 nm), and b is a calculated constant (0.0021 s^{-1}), which multiplies t and enters the equation as a negative exponent, $-\exp(-b \cdot t)$. The reciprocal of b (479 s ≈ 8 min) suggests that some factor (or factors) that accumulates or disappears with a half-life of about 8 min is controlling the cluster size. The aqueous hydrolysis of HAuCl$_4$ is an obvious candidate reaction, and it has a half-life of the order of 3−8 min under conditions close to those used in our delay-time procedure.[18]

A comparison of the total numbers and size distributions of preparations of oligoclusters made with different delay times shows that the number of oligoclusters formed decreases as the delay time lengthens while their diameters increase (see, for example, Figure 2A and B). This suggests that the well-known
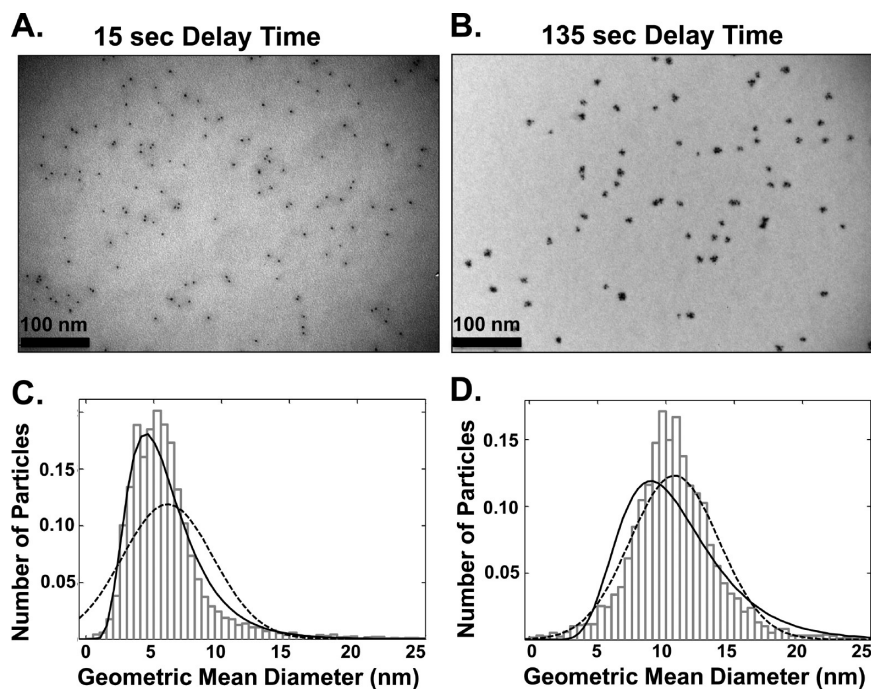

Figure 2. TEM determination of core sizes of oligoclusters and analysis of their distributions. (A and B) Representative TEM image of particles prepared with 15 and 135 s delay times. (C and D) Histograms of number of particles versus Feret diameters. The size distribution of the 15 s oligoclusters is close to log-normal (—). The 135 s oligoclusters are distributed close to normally (− − −).
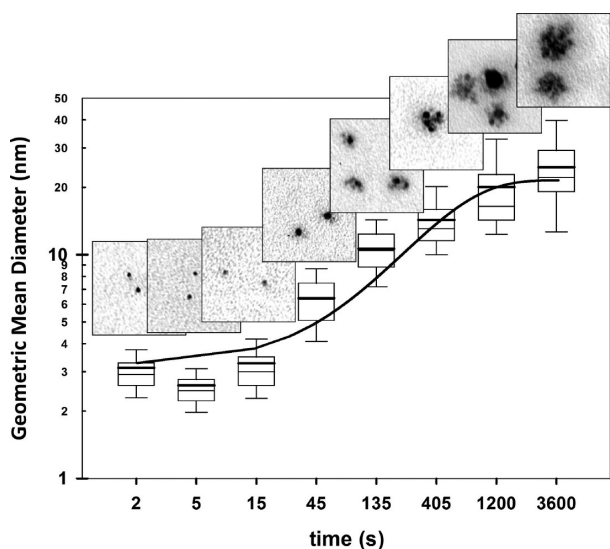
Figure 3. Diameters of gold oligoclusters formed after different delay times before adding NaSCN. Representative TEM images of 50 nm × 50 nm areas of grids prepared from the eight preparations used in the electrophoresis together with statistical data (box plots) for the sizes of the particles (Y axis) and the delay times used in their preparation (X axis). Both axes are logarithmic. The heavy and light lines within the boxes mark the mean and median core diameter. The upper and lower boundaries of the boxes are the 75th and 25th percentiles. Error bars are the 90th and 10th percentiles. The number of oligoclusters counted was 490, 2077, 385, 888, 2799, 1327, 1438, and 281 for the preparations made with 2, 5, 15, 45, 135, 405, 1200, and 3600 s delay times. The heavy black line ($R^2 = 0.973$) is a best-fit empirical three-parameter equation $f = y_0 + a \cdot (1 - \exp(-b \cdot t))$, where f is the mean diameter of clusters in nm, y_0 is the minimum diameter of clusters (~3.5 nm), a is the maximum increase in core size caused by extending the delay time (~20 nm), and b is 0.0021 s^{-1}. Because the parameter b is an exponent, the equation indicates that a factor (or factors) that is exponentially affected by time controls the increase in size of the oligoclusters.

Figure 4. Polyacrylamide gradient gel electrophoresis and TEM images of the products of the add-on procedure with different mixtures of seeds and HG. (A) Lane 1, 20 s seeds without HG (no HG); lanes 2−5, the products obtained after add-on reactions with 20 s seeds in the presence of 1/2×, 1×, 2×, and 4× HG. (B) Lane 1, the products of the add-on reaction with HG in the absence of seeds (No Seeds); lanes 2−4, 5−7, and 8−10, the products obtained with 5, 20, and 30 s seeds after add-on reactions with no HG, 1×, and 2× HG. Note that the overall sizes of the oligoclusters increase in proportion both to the sizes of the seeds and to the amount of HG. (C) TEM images of 30 s seeds without HG (no HG) and of the products of the add-on reaction in the presence of 1× HG and 4× HG, and with HG without added seeds (No Seeds). The black arrow points to oligoclusters that are too large to enter the gel.

alkaline hydrolysis of [AuCl$_4$]$^-$, a relatively slow equilibrium reaction with an initial half time of a few minutes,[15,16] converts [Au Cl$_4$]$^-$ into a form, "hydroxylated gold" (HG), that has a very limited ability or even a complete inability to generate new nucleation centers, but can still be reduced and add on to nucleation centers/nanoparticles which are already present.

3.3. Add-On Procedure. The inference that HG can contribute to the formation of oligoclusters in the presence of existing nanoparticles forms the basis of our "add-on" method of preparing oligoclusters in which sizes are controlled by mixing preformed nanoparticles (as seeds) with varying amounts of HG and adding NaSCN to complete the reduction.

As detailed in the Experimental Section, the add-on procedure starts with two stock solutions: (a) an aged 1 mM stock solution of HG, and (b) a preformed 1 mM stock solution of seeds of the desired size. The two stock solutions are mixed in various ratios, and 1 M NaSCN is added to give a final concentration of 10 mM. The mixes are kept overnight to allow the oligoclusters to develop.

The gel illustrated in Figure 4A compares the products obtained with 1 mM 20 s delay-time seeds and progressively increasing amounts of 1 mM HG. The average size of the oligoclusters increases as the relative amount of HG increases. The sizes of the oligoclusters are comparable to those obtained using the delay-time procedure; and the size distributions are as
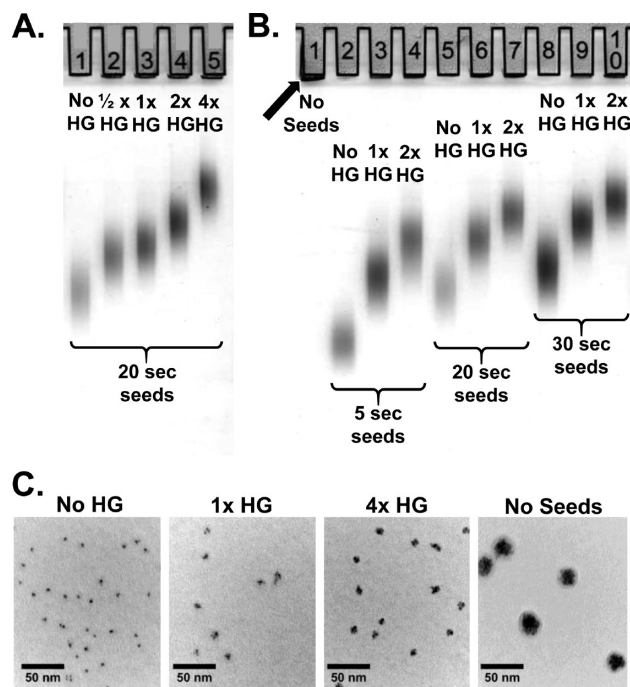
narrow. The gel in Figure 4B shows that HG can add-on to seeds of different sizes. Note that, in the presence of NaSCN, HG can still form oligoclusters without the addition of seeds, although the clusters are too large to enter this (4%) acrylamide gel (lane 1, No Seeds).

We conclude that equilibrium HG contains only a small amount of gold that can form effective seeds de novo in the presence of NaSCN, but that seeds catalyze the reduction of HG to elemental gold, which adds onto the seeds and also forms new nanoparticles that are integral parts of the final oligoclusters. The resulting oligoclusters are indistinguishable from those formed by the delay-time method. Figure 4C shows TEM images of the 30 s seeds without HG (No HG), clusters having only a few subunits when the ratio of seeds to HG was 1/1 (1× HG), larger clusters with more subunits when the ratio was 4/1 (4× HG), and very large clusters with many subunits formed in the absence of seeds (lane 1, No Seeds).

3.4. Stability of Oligoclusters. The oligoclusters proved to be highly stable; indeed, we were unable to find any conditions that caused them to revert to their subunits, and they could be prepared at 0 °C, room temperature, or 50 °C. GSH-derivatized oligoclusters made with 60 or 405 s delay times were not dissociated by exposure to 0.25 M GSH, 0.125 M GSH plus 0.125 M NaOH, 0.25 M NaSCN, 0.25 M NaHCO$_3$, or 1 M NaOH. Nor were they dissociated with 100
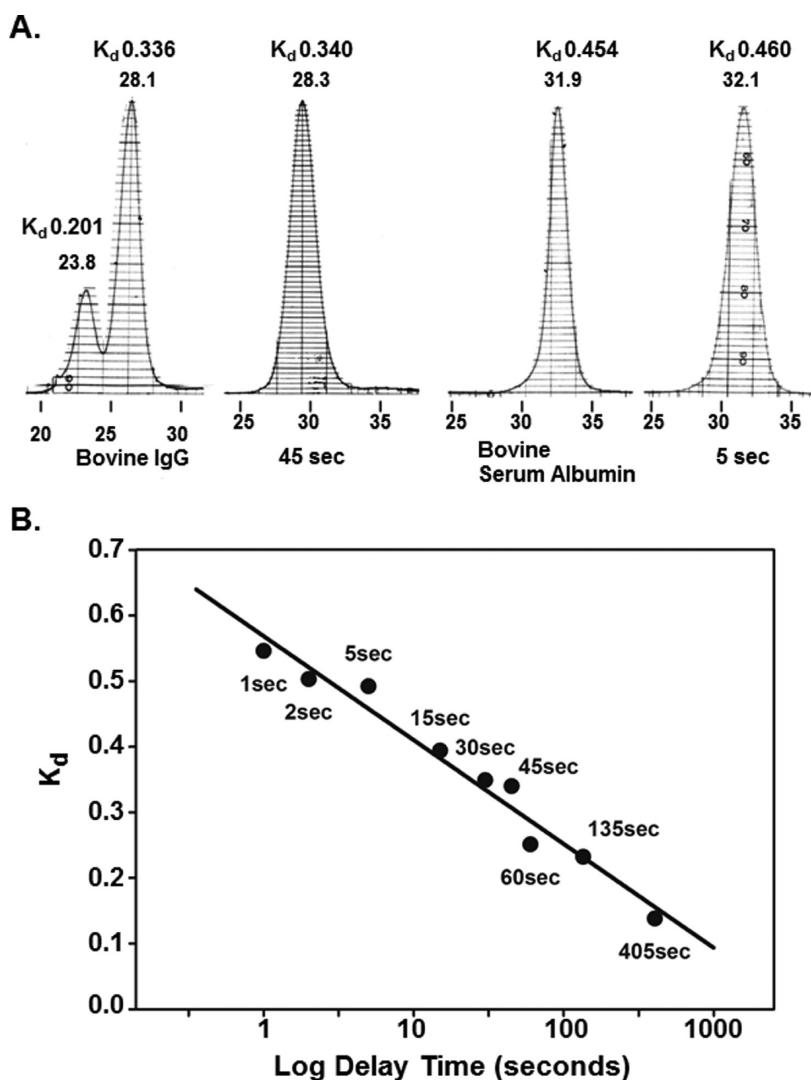
Figure 5. Hydrodynamic properties of oligoclusters prepared with different delay times. (A) Profiles of PBS elution from a Sephacryl S200 high-resolution 10/30 column of (left to right): purified bovine IgG, 45 s delay-time oligoclusters, bovine serum albumin, and 5 s delay-time oligoclusters. K_d, permeation coefficient; the numbers below the K_d's and on the horizontal axis are fraction numbers (0.5 mL/fraction). Absorption at 260 nm was used to detect the four eluents; vertical scales were adjusted to equalize peak heights and enable comparison of peak widths. (B) A plot of the permeation coefficients (K_d) of nine batches of oligoclusters against the logarithm of the delay time in seconds used in their preparation. The X axis is logarithmic.

mM KI plus 35 mM I_2 or 100 mM NaCN, reagents that can solubilize gold films.[19,20]

3.5. Gel Permeation Chromatography. The gel permeation properties of the oligoclusters prepared by the delay-time and add-on procedures were investigated and compared to the permeation properties of a series of purified proteins having different molecular weights and known Stokes' radiuses (Figure 5).

Figure 5A compares the elution profiles of purified bovine immunoglobulin (IgG) and bovine serum albumin with those of GSH-derivatized oligoclusters prepared with delay times of 45 and 5 s; the eluent was PBS; the column was packed with Sephacryl S200. As is apparent, the permeation coefficient (K_d) of the 45 s oligoclusters (0.340) is close to that of bovine IgG (0.336), and the K_d of the 5 s oligoclusters (0.460) is close to that of bovine serum albumin (0.454). The widths of the oligocluster peaks are narrow, not much greater than that of the purified proteins with similar K_d's, in agreement with the narrow size ranges of their gold cores documented in Figure 3.

Indeed, for most purposes, the size distribution is sufficiently narrow that the oligoclusters can be used without further purification. However, if desired, the derivatized oligoclusters can be concentrated and fractionated by Sephacryl S200 gel permeation chromatography.

Figure 5B shows that the permeation coefficients of oligoclusters prepared with different delay times decrease in proportion to the logarithm of the delay time. This supports the suggestion made above that a reaction occurring before the reductant is added reduces the number of de novo nucleation centers that the gold can generate after NaSCN is added, but does not prevent these fewer de novo centers from forming large sized oligoclusters. Note that the hydrodynamic radii of the GSH-modified oligoclusters are considerably larger than that of their gold cores. For example, the radius of the cores of the 5 s oligoclusters, as judged from TEM images, is ~1.5 nm, but the hydrodynamic radius of the same clusters is more than 10 times larger. This suggests that the GSH-derivatized oligoclusters have a high negative charge density and a large
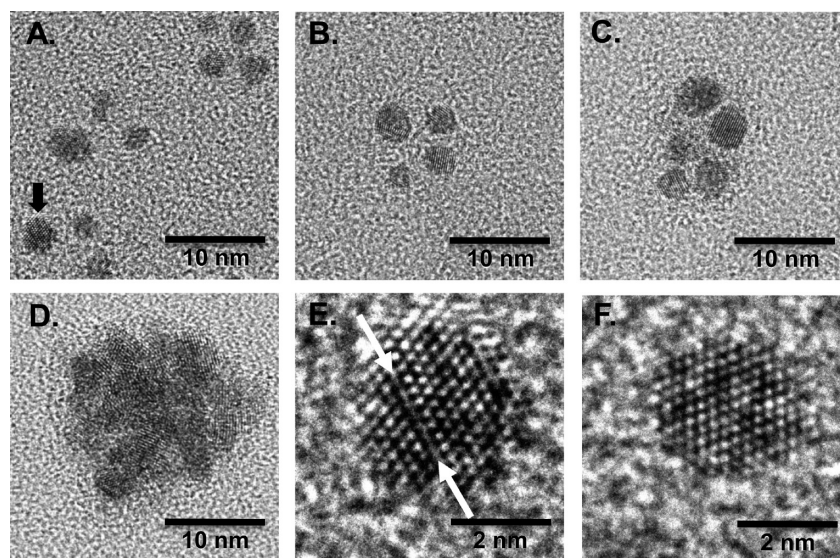
Figure 6. High-resolution transmission electron microscopy. (A) An image of several oligoclusters having 3 or 4 subunits in a sample prepared by the add-on method with a 1:1 mixture of 20 s seeds and HG. The arrow points to a subunit shown at higher magnification in panel E. (B) An image of a 4 subunit oligocluster in a sample prepared by the add-on method with a 1:1 mixture of 30 s seeds and HG. (C) An image of a 5 subunit oligocluster in a sample prepared by the add-on method with a 1:1 mixture of 135 s seeds and HG. An enlarged view of the subunit indicated by the arrowhead in panel A. (D) A very large oligocluster having about 50 subunits in a sample prepared by reducing HG in the absence of any seeds. (E) A higher magnification of the subunit in (A) indicated with a black arrow. The white arrows highlight a discontinuity in the crystal lattice, suggesting that the subunit is a twinned crystal formed by adding elemental gold onto a pre-existing particle. (F) A single nanoparticle in a sample prepared by the add-on method with a 1:1 mixture of 20 s seeds and HG.

positive ionic shell, which together prevent them from agglutinating even when they are at a high concentration in PBS, and protect them from binding plasma proteins when they are in the circulation. It may also account for the noticeable absence of aggregated material in TEM grids of the derivatized clusters (see, for example, panel C of Figure 4). Not surprisingly, the gel permeation of the oligoclusters derivatized with GSH is sensitive to the concentration of electrolytes in the eluent. Thus, the K_d's of the clusters decrease about 10% for every 2-fold decrease in the ionic strength of the eluent (Supporting Information Figure 1).

3.6. Surface Coats of the Oligoclusters. As expected from previous studies with conventional gold nanoparticles (reviewed by Briñas et al.),[21] derivatization of the oligoclusters to change their surface coats was readily obtained using the Murray place-exchange reaction[22] with a variety of thiol-containing reagents besides GSH. The resulting oligoclusters were resistant to aggregation by physiological buffers when derivatized with negatively charged thiols (2 mercaptoacetate, N-acetylcysteine), but not when the thiols were neutral (2 mercaptoethanol, dithiothreitol, cysteine) or positively charged (2 mercapto-ethylamine, cysteine ethylester). Other tested cysteine-containing peptides yielding PBS-resistant oligoclusters included CALNN and CALNNGK-biotinG[23] and CALNNGHHHHHHG (when mixed with CALNN). Derivatization with poly(ethylene) glycol-SH[24] or with tetra-(ethylene) glycol-SH[5] also yielded PBS-resistant oligoclusters. Mixed derivatization was readily accomplished with mixtures of thiols.

We investigated the effects of the different surface modifications on the hydrodynamic properties of oligoclusters prepared with a 60 s delay time. The simple negatively charged thiols tested (thioglycolic acid, N-acetyl cysteine, and penicill-amine) and negatively charged peptides (GSH and CALNN) had very similar effects on hydrodynamic sizes; their

permeation coefficients were within 10% of that of GSH-derivatized clusters. Derivatization of oligoclusters with poly-(ethylene glycol)-SH (PEG-SH 1000) greatly increased their hydrodynamic size; the permeation coefficient decreased to one-third that of GSH-derivatized clusters. In contrast, derivatization of oligoclusters with tetra(ethylene glycol)-SH (TEG-SH), while equally protective against aggregation, had only minimal effects on the hydrodynamic size of the clusters; the permeation coefficient was only 10% less than that of GSH-derivatized clusters. Additionally, TEG-SH decreased the negative charge of the clusters by ~25%.

Thus, the surfaces of the oligoclusters can be altered in many ways while still maintaining control of their hydrodynamic sizes.

3.7. High-Resolution Transmission Electron Microscopy. To better understand the add-on process, we obtained high-resolution transmission electron micrographs of clusters and subunits resulting from experiments in which the NaSCN reduction was carried out with or without seeds with or without hydrolyzed gold (HG). Figure 6A shows an image of several oligoclusters with 3 or 4 subunits when the add-on reaction was carried out with a 1:1 mixtures of HG and 20 s delay-time seeds. Note the wide separation of the subunits. Nothing sufficiently electron dense to be visualized in the TEM image is apparent between the subunits, although the remarkable stability of the oligoclusters suggests that some covalently bonded polymeric chain is linking them.

Figure 6B and C shows images of oligoclusters with 4 and 5 subunits formed when the add-on reaction was carried out with 1:1 mixtures of HG and 30 s (Figure 6A) and 135 s (Figure 6B) delay-time seeds. Note that the packing of the subunits appears closer in the 5 subunit oligocluster than in the 3 subunit oligoclusters. Figure 6D shows an image of a very large oligocluster with about 50 subunits from a sample prepared by NaSCN reduction of HG in the absence of any seeds. As expected, the oligocluster is much larger than that formed in

the presence of seeds and contains many more subunits. The sizes of the subunits are not obviously different from those comprising the small oligoclusters, although the subunits in the large oligocluster are more closely packed with little space between them. Nevertheless, the images are compatible with our inference that the overall sizes of the oligoclusters depend mainly on the number of subunits that they contain. Figure 6E shows that one of the subunits of the oligoclusters in Figure 6A was twinned, as indicated by the discontinuity highlighted with white arrows. Such twinned crystals were seen quite frequently in the products of the add-on reaction. They were also seen at a lower frequency in the products of delay-time reactions, probably formed by add on with hydrolyzed gold that continues to be formed even after the addition of NaSCN. We conclude that nanoparticles formed in the delay-time procedure, or introduced as seeds in the add-on procedure, can provide foci onto which elemental gold derived from HG is deposited. Figure 6F shows a single crystal from a preparation made with a delay time of 20 s. The nanocrystal is estimated to contain about 1000 gold atoms, which are as close packed as the gold atoms in gold metal.

3.8. Urinary Excretion of Oligoclusters.
An important feature of our oligoclusters is that their sizes can be controlled to allow or prevent their excretion by the kidney. This capability is illustrated in Figure 7, which presents the results of
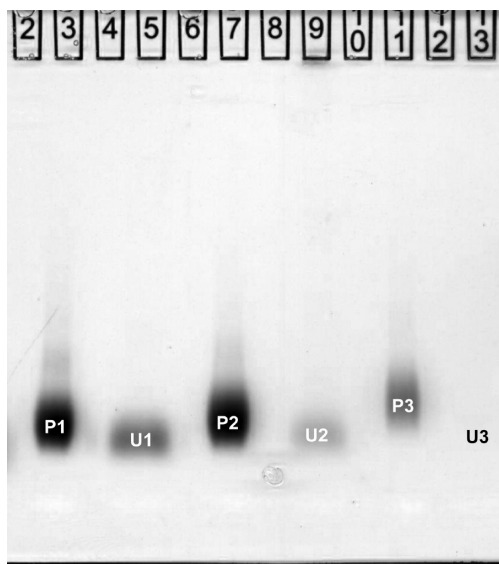

Figure 7. Urinary excretion of small injected oligoclusters. Gradient gel electrophoresis of three oligocluster preparations (P1, P2, and P3) made with delay times of 1, 2, and 5 s and derivatized with GSH. Approximately 5 min after injecting the preparations intravenously into mice, urine samples were collected from their bladders, processed as described in the Experimental Section, and run (as U1, U2, and U3) alongside samples of the corresponding injected material.

experiments in which unfractionated preparations of GSH-modified oligoclusters made with different delay times (1, 2, and 5 s) were injected intravenously into mice, and their excretion in the urine was determined by comparing the gel electrophoretic behavior of the injected and excreted materials.

The gel shows that, as judged by their faster migrations in the gradient gel, smaller particles present in the unfractionated injected material reached the urine (U1 and U2) of the mice receiving 1 or 2 s delay-time preparations (P1 and P2) but

larger sized clusters in the same preparations did not. In contrast, because most of the particles in the unfractionated 5 s delay preparation (P3) are larger than those in U1 and U2, almost none of them were excreted in the urine (U3). As shown in Figure 5, the 5 s delay-time clusters have an average permeation coefficient (0.460) close to that of albumin (0.454). Because in normal mice and humans albumin reaches the urine in only small amounts, the absence of the 5 s delay clusters from the urine is to be expected. In contrast, the 1 s delay oligoclusters are expected to reach the urine, because their average permeation coefficient (0.602) is a little greater than that of ovalbumin (0.546), which is known to pass the renal glomerular barrier.[25] We conclude that the sizes of the oligoclusters can be controlled to allow or prevent their excretion in the urine.

3.9. Retention of Oligoclusters in the Circulation.
In the other direction, the sizes of the oligoclusters can be made so large that they cannot pass through basement membranes but are still not aggregated in the bloodstream. Figure 8 illustrates this capability by showing that oligoclusters made with a 405 s delay time are largely excluded from the basement membrane of the renal glomerulus, although they are clearly well dispersed and free from aggregation in the plasma. Because the number of particles per image is about 100 times greater than has previously been possible, and many images can be examined and the data combined, it should be possible to detect and quantify permeation into the GBM at levels as low as 0.01 times that in plasma.

3.10. Toxicity.
The GSH-coated oligoclusters show no evidence of acute toxicity as judged by the absence of any visible distress in mice receiving them intravenously by tail vein as compared to mice receiving PBS. Long-term effects remain to be determined.

3.11. Reaction Mechanism.
The thiocyanate reduction of Au(III) to Au(I) in acidic solutions of $HAuCl_4$ has been extensively investigated by Bjerrum and Kirschner and Elding et al.[26,27] The first step is an extremely rapid substitution/displacement of Cl by SCN leading to dark red $HAu(SCN)_4$. The second step is a slower but still very rapid reduction of Au(III) to Au(I) by free solution thiocyanate leading to colorless NCS-Au-SCN and the formation of thiocyanogen $(SCN)_2$, which more slowly decomposes to give $HSO4^-$ and HCN. The overall reaction can be represented stoichiometrically by eq 1.

$$3(AuCl_4)^- + 7SCN^- + 4H_2O$$
$$\rightarrow 3[Au(SCN)_2]^- + HSO_4^- + HCN + 12Cl^- + 6H^+ \tag{1}$$
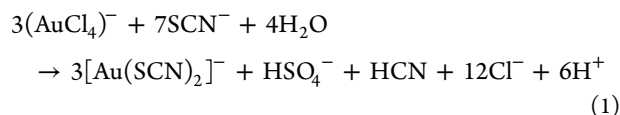
Elding et al.[27] state that the reduction is rapid and complete when the gold concentration is ≤ 5 nM and that the Au(I) formed by the reduction is present as $[Au(SCN)_2]^-$. At higher gold concentrations (0.1−1 mM), cyanide resulting from the hydrolysis of thiocyanogen forms cyanide complexes that are reduced very slowly by thiocyanate. Thus, the initial very high rate of reduction decreases more than 1000-fold as HCN is formed. In our hands, no further reactions occur at an acidic pH when the final concentrations of gold and thiocyanate are, respectively, ~1 and ~10 mM. The solution remains clear and colorless for weeks; no nanoparticles are formed and no gold precipitates develop. Even if this acidic solution is made alkaline, no nanoparticles develop, although traces of a fine gold precipitate are formed. We conclude that the end-product of
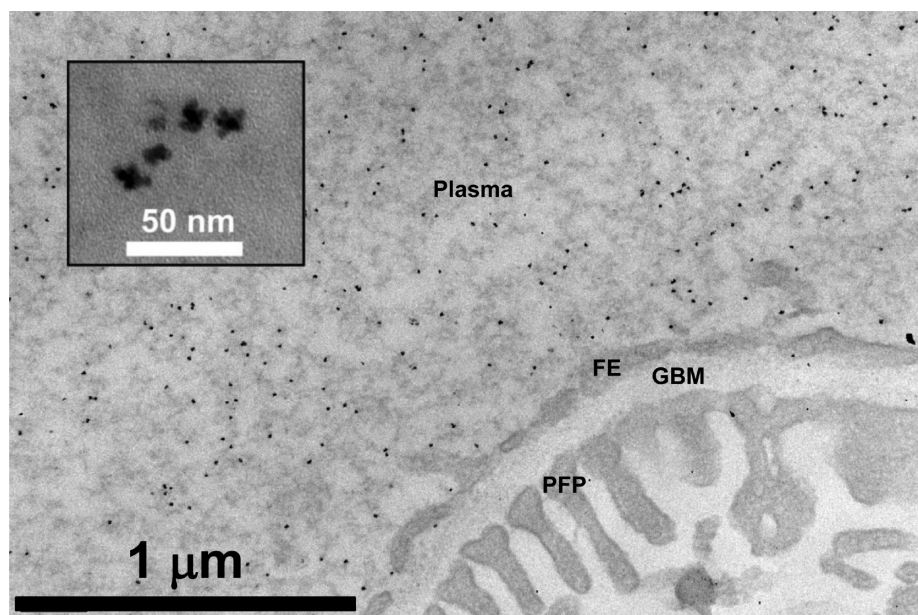
Figure 8. Retention in the circulation of large injected oligoclusters. TEM image of renal glomerulus after intra-arterial injection of oligoclusters made with a delay time of 405 s. Inset: A higher magnification of oligoclusters present in the plasma. GBM, glomerular basement membrane; FE, fenestrated endothelium; PFP, podocyte foot process. Note that none of the oligoclusters have penetrated the basement membrane and that, despite their large size, they do not aggregate in the plasma. The dark spot in the image at 4 o'clock from "GBM" is a camera artifact, not an oligocluster.

the acidic reaction, $[Au(SCN)_{2-n}(CN)_n]^-$, where n is ≤ 2, does not disproportionate in aqueous solution. This finding is in general agreement with previous work indicating that electron transfer along the -Au- axis occurs most readily when the two ligands have a large difference in their ground-state *trans* influence.[28] Further support for the conclusion that the product of the acidic reaction does not disproportionate is provided by our finding that it is unable to serve as a source of gold for the add-on procedure.

In contrast, if the $HAuCl_4$ is first made alkaline and then exposed to thiocyanate, as described by Baschong et al.,[12] the reduction to Au(I) is followed rapidly by a disproportionation/autoreduction reaction (eq 2)[29] leading to the formation of large numbers of yellow 2−3 nm diameter nanoparticles.

$$3[AuCl_2]^- = 2Au + [AuCl_4]^- + 2Cl^- \qquad (2)$$
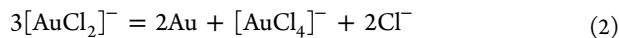
The development of the nanoparticles is already apparent within a few minutes, although it takes hours to go to completion. Previous investigators have clearly established that when gold chloride is made alkaline, hydroxyl ions displace chloride.[15,16] The reaction favors hydroxylation but is reversible. Equilibrium is reached after a few days with the formation of mixtures of partially and completely hydroxylated Au(III), represented as $[AuCl_{4-n}(OH)_n]^-$. Although n approaches 4 at higher pH, some $[AuCl(OH)_3]^-$ is still present even at pH > 10. As described above, our experiments show that after the hydrolysis has come to equilibrium, the resulting hydroxylated gold (HG) can still form particles when thiocyanate is added, but the reaction is slow and the resulting particles are very large oligoclusters comprised of ∼50 subunits. Our delay-time procedure for preparing oligoclusters of different sizes takes advantage of the relatively slow rate of the hydroxylation. Thus, with delay times of seconds, many oligoclusters are formed, each having only small numbers of subunits, while with longer delay times fewer oligoclusters are formed, but they have more subunits. We hypothesize that

thiocyanate is unable to generate nucleation centers from fully hydroxylated $[Au(OH)_4]^-$, perhaps because the reaction only proceeds at an appreciable rate when an asymmetric species is present.[28] However, if preformed nanoparticles are added as seeds, they catalyze the NaSCN reduction of $[Au(OH)_4]^-$ to Au, which adds on to the seeds and also forms new subunits that are integral parts of the resulting oligoclusters, as illustrated above by high-resolution TEM images.

The catalytic effects of gold flakes, or in our case preformed gold nanoparticles, on the thiocyanate reduction of $HAuCl_4$ have been noted by others.[26,27,30] Gammons et al.[30] hypothesize that metallic gold catalyzes the disproportionation reaction by mediating the transfer of electrons between adsorbed reactants. This would enable participating reactants to disproportionate even when their concentrations are so low that bimolecular collisions between them are unlikely to occur in solution. Because the disproportion reaction regenerates $[AuCl_4]^-$, and this can be reduced by NaSCN (which is present in excess), repeated cycles of this solid phase catalysis could allow the reduction of HG to go to completion even though HG contains very little unhydroxylated gold. In the delay-time procedure, the hydroxylation of Au(III) begins before any reductant is added, but there is still sufficient unhydroxylated gold present after the delay for the uncatalyzed de novo formation of nanoparticles to occur when the NaSCN is added; both the uncatalyzed de novo formation of nanoparticles and the catalyzed capture of HG continue until all of the gold is fully reduced. In the add-on procedure, the hydroxylation, the formation of catalytically active seeds, and the catalyzed capture of HG are separated, and the composition of the oligoclusters can therefore be more precisely controlled.

The cartoon in Figure 9 summarizes our observations. The sizes of the oligoclusters depend on the number of subunits (n) that they contain. The number of oligoclusters formed (N) is a reflection of the number of discrete nucleation centers that form in the delay-time reaction, or are added as seeds in the
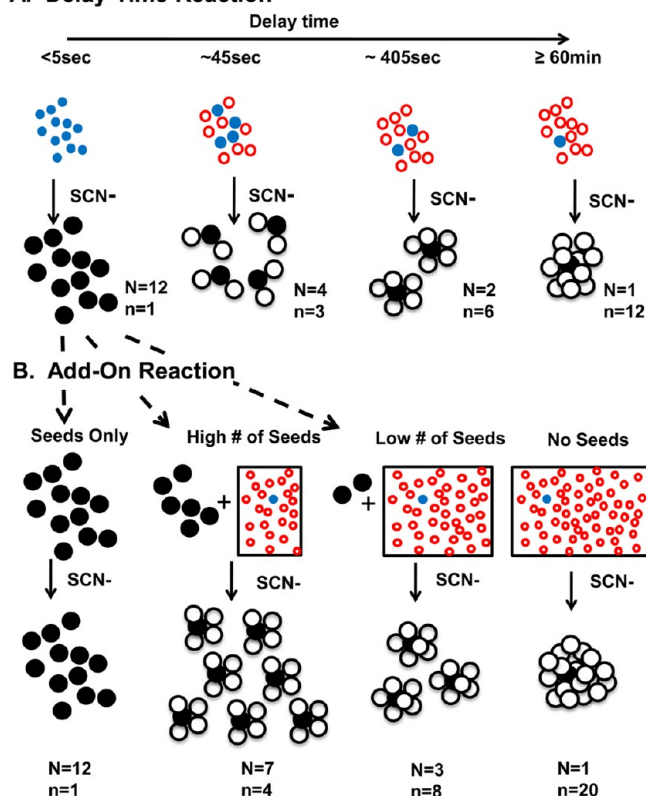
Figure 9. Schematics of delay-time reaction (A) and add-on reaction (B). (A) Delay-time reaction. After $HAuCl_4$ is made alkaline, species that are able to nucleate (blue ●) are progressively converted by hydrolysis into species that are unable to nucleate (red ○) but are able to add on to existing particles. Addition of SCN^- initiates the nucleation and growth processes. In reactions with delay times less than 5 s, almost all species present are able to nucleate, and the reduction/growth processes continue until all of the gold is reduced and the particles reach the stable size (●), characteristic of the reduction of gold chloride by NaSCN under alkaline conditions. In reactions with longer delay times, nucleation-unable species are present, which can only be reduced by catalysis resulting from contact with already existing nucleation centers or fully formed nanoparticles. All subunits, including those formed by contact catalysis (○), can catalyze the formation and growth of additional subunits using any unreduced gold remaining in the mix. The number of oligoclusters formed (N) decreases with longer delay times, because hydrolysis decreases the amount of nucleation-able species present when the NaSCN reduction is initiated. The number of subunits in the resulting oligoclusters (n) depends on the total amount of blue "●" plus red "○" present in the reaction mix. Because this is normally kept fixed at 1 mM, $N \times n$ is constant regardless of the delay time. (B) Add-on reaction. In this reaction, the hydrolytic process is separated from the reduction/growth processes. Preformed nanoparticles, "●", are used as seeds. Fully hydrolyzed nucleation-unable species, red "○", are used as sources of additional gold that by contact catalysis can form additional subunits, "○". Thus, the number of oligoclusters, N, formed is determined by the number of seeds present in the reaction mix, while the number of subunits in the resulting oligoclusters, n, increases as N decreases, since the total amount of gold in the reaction mix is kept constant.

add-on reaction. The total number of subunits formed ($N \times n$) is determined by the total amount of gold present in the reaction, which is kept constant. The two methods provide different ways of controlling the number of effective nucleation centers (the number of oligoclusters) and thence the number of subunits that they contain.

4. CONCLUSION/SUMMARY

The oligoclusters prepared by either the delay-time or the add-on procedure have a wide range of interesting and useful properties, summarized as follows:

(1) The oligoclusters are chemically bonded clusters of crystalline subunits.

(2) The oligoclusters are extremely difficult to disrupt physically or chemically.

(3) The number of subunits in the oligoclusters is controllable over a >50-fold range.

(4) The size distribution of the oligoclusters in all preparations is narrow, and they can be used for most purposes without further fractionation.

(5) The electron densities of the oligoclusters combined with their unique form make them easy to recognize in the TEM without enhancement, and they are consequently useful for following the fate of differently sized or differently charged macromolecules at subcellular levels.

(6) The large and small oligoclusters have sufficiently distinct TEM images that mixtures can be used to uncover subtle size-dependent differences in behavior.

(7) Crude underivatized preparations of the oligoclusters can be concentrated several hundred fold without them precipitating.

(8) The concentrated oligoclusters can be derivatized with numerous thiol-containing reagents.

(9) When derivatized with GSH or other cysteine-containing peptides, they have a surface comparable to proteins, making them useful protein-like models for a variety of studies.

(10) Because the oligoclusters can be concentrated before derivatization, expensive or rare derivatizing reagents can be used economically.

(11) Mixed derivatization is readily accomplished.

(12) The oligoclusters, whether large or small, are resistant to aggregation by PBS or by plasma.

(13) Mice receiving them intravenously at high concentrations show no visible signs of distress.

(14) The hydrodynamic sizes of the oligoclusters can be made small enough to allow their excretion by the kidney or so large that they do not pass through basement membranes.

(15) This property combined with the ease of modifying their coats with mixed reagents makes the oligoclusters potentially useful for presenting pharmacological agents to different tissues while controlling escape of the reagents from the circulation.

■ ASSOCIATED CONTENT

Ⓢ Supporting Information

Effect of ionic strength on K_d. This material is available free of charge via the Internet at http://pubs.acs.org.

■ AUTHOR INFORMATION

Corresponding Authors
*E-mail: oliver_smithies@med.unc.edu.
*E-mail: tilen.koklic@ijs.si.

Present Addresses
∥Department of Chemistry, Murray State University, Murray, Kentucky 42071, United States.

[1]Department of Virology, Imperial College London, South Kensington Campus London, London SW7 2AZ, United Kingdom.

Notes

The authors declare no competing financial interest.

ABBREVIATIONS

NaSCN, sodium thiocyanate; PBS, phosphate-buffered saline; TEM, transmission electron microscopy; $HAuCl_4$, chloroauric acid; GSH, glutathione; $NaBH_4$, sodium borohydride; $Na_2B_4O_7 \cdot 10H_2O$, borax; HG, "hydroxylated gold"; HCN, hydrogen cyanide; HRTEM, high-resolution transmission electron microscopy; CALNN, a pentapeptide ligand, which converts gold nanoparticles into stable, water-soluble nanoparticles; GBM, glomerular basement membrane; FE, fenestrated endothelium; PFP, podocyte foot process

REFERENCES

(1) Heim, R.; Prasher, D. C.; Tsien, R. Y. Wavelength Mutations and Posttranslational Autoxidation of Green Fluorescent Protein. *Proc. Natl. Acad. Sci. U.S.A.* **1994**, *91*, 12501–12504.

(2) Farquhar, M. G.; Wissig, S. L.; Palade, G. E. Glomerular Permeability. I. Ferritin Transfer across the Normal Glomerular Capillary Wall. *J. Exp. Med.* **1961**, *113*, 47–66.

(3) Sterzel, R. B.; Perfetto, M.; Biemesderfer, D.; Kashgarian, M. Disposal of Ferritin in the Glomerular Mesangium of Rats. *Kidney Int.* **1983**, *23*, 480–488.

(4) Jarad, G.; Cunningham, J.; Shaw, A. S.; Miner, J. H. Proteinuria Precedes Podocyte Abnormalities inLamb2-/- Mice, Implicating the Glomerular Basement Membrane as an Albumin Barrier. *J. Clin. Invest.* **2006**, *116*, 2272–2279.

(5) Bartz, M.; Küther, J.; Nelles, G.; Weber, N.; Seshadri, R.; Tremel, W. Monothiols Derived from Glycols as Agents for Stabilizing Gold Colloids in Water: Synthesis, Self-Assembly and Use as Crystallization Templates. *J. Mater. Chem.* **1999**, *9*, 1121–1125.

(6) Hainfeld, J. F.; Slatkin, D. N.; Focella, T. M.; Smilowitz, H. M. Gold Nanoparticles: A New X-Ray Contrast Agent. *Br. J. Radiol.* **2006**, *79*, 248–253.

(7) Paciotti, G. F.; Myer, L.; Weinreich, D.; Goia, D.; Pavel, N.; McLaughlin, R. E.; Tamarkin, L. Colloidal Gold: A Novel Nanoparticle Vector for Tumor Directed Drug Delivery. *Drug Delivery* **2004**, *11*, 169–183.

(8) Khlebtsov, N.; Dykman, L. Biodistribution and Toxicity of Engineered Gold Nanoparticles: A Review of in Vitro and in Vivo Studies. *Chem. Soc. Rev.* **2011**, *40*, 1647–1671.

(9) Kumar, A.; Zhang, X.; Liang, X.-J. Gold Nanoparticles: Emerging Paradigm for Targeted Drug Delivery System. *Biotechnol. Adv.* **2013**, *31*, 593–606.

(10) Schaaff, T. G.; Knight, G.; Shafigullin, M. N.; Borkman, R. F.; Whetten, R. L. Isolation and Selected Properties of a 10.4 kDa Gold:Glutathione Cluster Compound. *J. Phys. Chem. B* **1998**, *102*, 10643–10646.

(11) De Brouckere, L.; Casimir, J. Preparation D'hydrosols D'or Homesdisperses Tres Stable. *Bull. Soc. Chim. Belg.* **1948**, *57*, 517–524.

(12) Baschong, W.; Lucocq, J. M.; Roth, J. Thiocyanate Gold: Small (2-3 nm) Colloidal Gold for Affinity Cytochemical Labeling in Electron Microscopy. *Histochemistry* **1985**, *83*, 409–411.

(13) Capretta, P. J. Saccharin and Saccharin-Glucose Ingestion in Two Inbred Strains of Mus Musculus. *Psychon. Sci.* **2013**, *21*, 133–135.

(14) Cook, M. J. *The Anatomy of the Laboratory Mouse*; Academic Press: New York, 1965; Vol. 14, p 143.

(15) Wang, S.; Qian, K.; Bi, X.; Huang, W. Influence of Speciation of Aqueous HAuCl 4 on the Synthesis, Structure, and Property of Au Colloids. *J. Phys. Chem. C* **2009**, *113*, 6505–6510.

(16) Britton, H. T. S.; Dodd, E. N. Electrometric Studies of the Precipitation of Hydroxides. Part V. Tervalent Gold Chloride Solutions. *J. Chem. Soc.* **1932**, 2464.

(17) Rance, G. A.; Marsh, D. H.; Khlobystov, A. N. Extinction Coefficient Analysis of Small Alkanethiolate-Stabilised Gold Nanoparticles. *Chem. Phys. Lett.* **2008**, *460*, 230–236.

(18) Fry, F. H.; Hamilton, G. A.; Turkevich, J. The Kinetics and Mechanism of Hydrolysis of Tetrachloroaurate(III). *Inorg. Chem.* **1966**, *5*, 1943–1946.

(19) Davis, A.; Tran, T. Gold Dissolution in Iodide Electrolytes. *Hydrometallurgy* **1991**, *26*, 163–177.

(20) Templeton, A. C.; Chen, S.; Gross, S. M.; Murray, R. W. Water-Soluble, Isolable Gold Clusters Protected by Tiopronin and Coenzyme A Monolayers. *Langmuir* **1999**, *15*, 66–76.

(21) Briñas, R. P.; Maetani, M.; Barchi, J. J. A Survey of Place-Exchange Reaction for the Preparation of Water-Soluble Gold Nanoparticles. *J. Colloid Interface Sci.* **2013**, *392*, 415–421.

(22) Hostetler, M. J.; Green, S. J.; Stokes, J. J.; Murray, R. W. Monolayers in Three Dimensions: Synthesis and Electrochemistry of Ω-Functionalized Alkanethiolate-Stabilized Gold Cluster Compounds. *J. Am. Chem. Soc.* **1996**, *7863*, 4212–4213.

(23) Lévy, R.; Thanh, N. T. K.; Doty, R. C.; Hussain, I.; Nichols, R. J.; Schiffrin, D. J.; Brust, M.; Fernig, D. G. Rational and Combinatorial Design of Peptide Capping Ligands for Gold Nanoparticles. *J. Am. Chem. Soc.* **2004**, *126*, 10076–10084.

(24) Wuelfing, W. P.; Gross, S. M.; Miles, D. T.; Murray, R. W. Nanometer Gold Clusters Protected by Surface-Bound Monolayers of Thiolated Poly(ethylene Glycol) Polymer Electrolyte. *J. Am. Chem. Soc.* **1998**, *120*, 12696–12697.

(25) Lemley, K. V. Glomerular Size Selectivity during Protein Overload in the Rat. *Am. J. Physiol.* **1993**, *264*, F1046–51.

(26) Bjerrum, N.; Kirschner, A. Thiocyanates of Gold and Free Cyanogen. *Kgl. Danske Vidensk. Selsk.* **1918**, *V*, 78.

(27) Elding, L. J.; Groning, A. .; Gronig, O. Kinetics and Mechanisms of Reaction between Tetrachloro- and Tetrabromo-aurate(III) and Thiocyanate. *J. Chem. Soc., Dalton Trans.* **1981**, 1093–1100.

(28) Elmroth, S. K. C.; Elding, L. I. Competitive Substitution and Electron Transfer in Reactions between Haloamminegold(III) and Halocyanoaurate(III) Complexes and Thiocyanate. *Inorg. Chem.* **1996**, *35*, 2337–2342.

(29) Lingane, J. J. Standard Potentials of Half-Reactions Involving + 1 and + 3 Gold in Chloride Medium. *J. Electroanal. Chem.* **1962**, *4*, 332–342.

(30) Gammons, C. H.; Yu, Y.; Williams-Jones, A. E. The Disproportionation of gold(I) Chloride Complexes at 25 to 200 °C. *Geochim. Cosmochim. Acta* **1997**, *61*, 1971–1983.